Effect of Posture on Subcutaneous Adipose Tissue: A Preliminary Imaging Study

A. S. Robinson[1,2], S. Efobi[2], J. Aira[2], A. Moore[1,2], L. Lenchik,[1] A. A. Weaver[1,2], F. Hsu[1], J. Hallman[3], F. S. Gayzik[1,2]

[1] Wake Forest University School of Medicine; [2] Virginia Tech-Wake Forest Center for Injury Biomechanics; [3]Toyota Motor North America CRSC.

ABSTRACT

The potential rise of autonomous vehicles has prompted studies of occupants in reclined seating positions. However, the anatomic morphology of subcutaneous adipose tissue (SAT) in the region of the anterior superior iliac spine (ASIS) in reclined postures is not well understood. The current study builds off of previous work characterizing the morphology of SAT in this region using supine CT data. The objective of this study was to investigate how measures of SAT are affected by image modality and posture. A retrospective study of matched supine CT, supine MRI, and seated MRI scans (at 23 degree seatback angle) from 6 living subjects was conducted, and eleven measurements describing area, quality, and linear depth were collected from each scan. SAT measures were found to correlate well between CT and MRI in the supine posture, while variation was found when analyzing supine scans (CT or MRI) vs. seated MRI scans. When assessing postural changes, area remains unchanged from supine to seated posture, yet significant differences were observed ASIS depth measures from the supine to seated posture. The results therefore suggest the shortcomings of using supine data to develop human body models in seated and reclined settings. This study indicates the need for further analysis, and a need for more robust imaging data describing SAT morphology with variation in the seated posture.

INTRODUCTION

Computational human body models (HBMs) are widely used to investigate injury risk and mechanisms associated with motor vehicle crashes. The emergence of autonomous vehicles makes reclined seating postures a potential area for further study, so that occupant safety in this environment can be better understood. Recent studies on HBMs and Post-Mortem Human Subjects (PMHS) have identified a specific need to better understand the biomechanical behavior of subcutaneous adipose tissue (SAT) in the region of the anterior superior iliac spine (ASIS) (Luet et al. 2012; Lamielle et al. 2006). In the case of modeling, understanding the biomechanics begins with well characterized in situ morphology.

PMHS studies in reclined seating postures have begun to examine restraint performance and were used to develop response corridors for HBM model validation (Richardson et al. 2019;

Uriot et al. 2015; Luet et al. 2012). Furthermore, HBMs have been used in to better understand injury tolerance in the reclined seating environment (Boyle et al. 2019; Rawska et al. 2019; Gepner et al. 2019). However, imaging data of PMHS are typically not collected in a seated posture. Measures of SAT in the ASIS region in reclined settings are necessary to accurately model the interaction of the lap belt with the body.

Therefore, the current study builds off of previous work characterizing the morphology of SAT in this region using supine CT data. The objective is twofold. First, we seek to establish correspondence between measures of SAT in matched abdominal CT and MRI scans from the same individuals in the supine posture. Next, we seek to expand that analysis by comparing data from the same individuals in a seated posture.

METHODS

Study Population

The study population for this project was n = 6 subjects (Table 1). The image data and protocol have been previously described in the literature (Gayzik et al. 2011; Gayzik et al. 2012; Gayzik et al. 2009). The data were collected previously for the purpose of human body model development.

Table 1. Metadata for study population

ID	Gender	Height (cm)	Weight (kg)	BMI	Age (years)
M05	M	160.02	57.658	22.517	27
M50	M	175.26	78.542	25.570	26
M95	M	189.5475	97.61	27.168	26
F05	F	149.86	46.762	20.822	24
F50	F	162.56	59.02	22.334	31
F95	F	167.005	90.8	32.556	33

Image Reslicing and Preparation

Images were downloaded from the WFU PACS (Picture Archiving and Communication System) and loaded in Mimics v23.0 (Materialise, Leuven, Belgium). To correct pelvic tilt or rotation due to patient positioning, each scan was resliced in order to reorient the images to the anatomical axes of the pelvis (Figure 1).

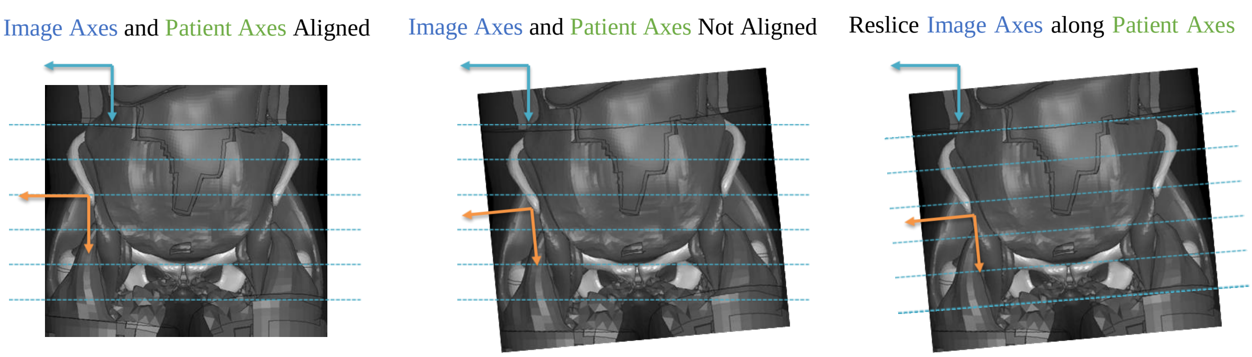

Figure 1. Reslicing protocol to align image axes to patient axes.

The reslicing process leveraged the left and right ASIS and pubic symphysis to establish a coronal plane through these landmarks (Figure 2). All analysis was conducted in a plane perpendicular to this baseline coronal plane, through the subjects' ASIS. In instances where the pubic symphysis was not visible in MRIs, the orthogonal plane was used instead. This plane was aligned to the sacrum, matching the same landmarks observed in the CT where the pubic symphysis was visible and resliced according to normal protocol.

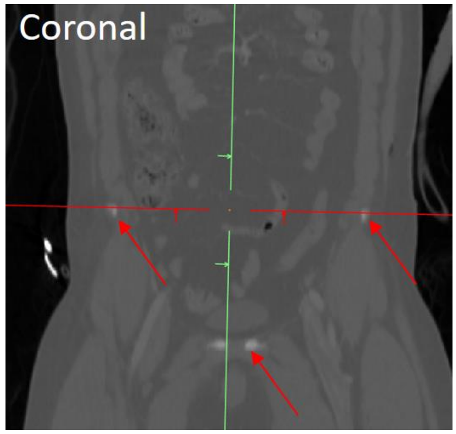

Figure 2. Exemplar coronal plane used to establish analysis plane.

Image Analysis

The data collected on the scans can be broken into two categories: SAT area and quality measures or SAT linear depth measures. Methods to determine each are discussed below. The use of existing medical images in this study is authorized under the IRB protocol IRB00013200 at Wake Forest School of Medicine for retrospective analysis.

SAT Area and Quality

Segmentation of visualized anatomical structures was done using Mimics v23 (Materialise, Leuven, Belgium). SAT area was determined semi-automatically. For CTs a thresholding operation was used to select pixels within the range of Hounsfield Units (HU) commonly associated with SAT (HU = -150 to -40). A thresholding operation was used for MRI and uMRI as well, but the HU range was adjusted to best match SAT. Following this, scans were manually edited to remove voxels at skin, viscera, and to fill in any voids surrounded by SAT. The collection of voxels (aka a *mask*) was then used to calculate volume, number of voxels, and average HU within the mask. Based on each image slice thickness, the area was calculated by dividing the mask volume by the slice thickness. Fat quality was assessed by documenting the mean of the HU value of the mask. A border was drawn around the outer surface of skin and was used to establish measures of perimeter, perpendicular diameter, and maximum diameter.

Tissue Depth and Linear Measures

Linear measures were collected using Mimics v23 (Materialise, Leuven, Belgium). An axis of symmetry was drawn through the linea alba anteriorly, and middle of sacrum posteriorly. Next, a vector was placed through anterior aspect of the sacroiliac (SI) joint and the ASIS bilaterally. This vector was used to then establish three measures of SAT depth at the ASIS: Along line from SI, Lateral (traditionally thought of as the “Y” axis depth for SAE J211), anterior-posterior (traditionally thought of as the “X” axis depth for SAE J211). Depth was also measured at 3 other locations, normal to the external surface of the skin: bilaterally at the arcuate line (distal border of rectus abdominis muscle, right and left) and along midline at linea alba (navel).

Additional Sagittal Measurements

For all scans, additional measurements were taken to evaluate how sensitive measured linea alba depth was to the plane in which data were taken per-protocol. When in a seated posture, natural folding of a pannus could present variable SAT thickness, but it is also possible for clothing, such as an elastic waistband or belt, to locally deform the SAT. Additional depths were collected from seated MRIs in the sagittal plane. These measurements were superior to and inferior to the per-protocol measurement collected at the level of the ASIS. The distance from the original measurement was chosen to best represent the range of depths as seen in the scans. A depiction of these measurements is shown in Figure 3.

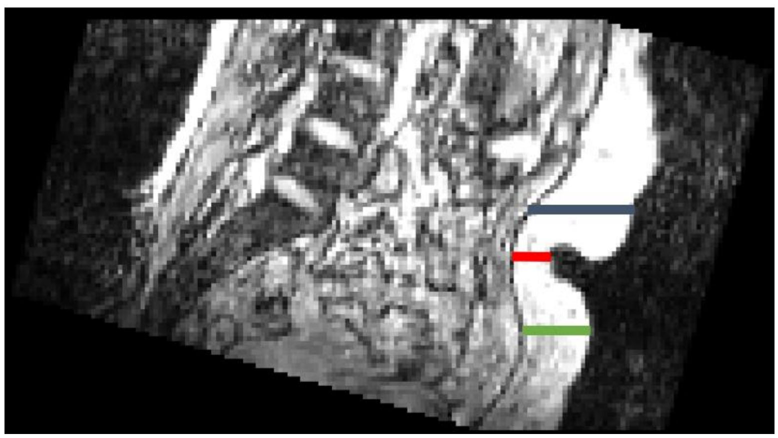

Figure 3. Example of SAT fold in sagittal view. Depiction of the original depth at linea alba measurement is shown in red with additional measurements above (gray) and below (green).

Outcome Measures

A summary of the outcome measures is shown below in Table 2. Measurements were collected for CT, MRI, and uMRI scans.

Table 2. SAT measurements taken from scan data

Measurement	Image	Measurement	Image
Lumbar lordosis, Curvature of the spine as measured from L1 to sacrum	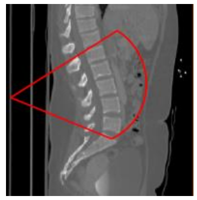	**$ASIS_{Ant}$ depth**, Anterior component of depth of SAT as measured along a vector from SI joint to ASIS in plane (R,L)	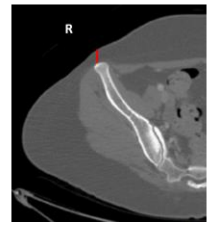
Mean HU value, Average gray scale value noted in the segmented SAT	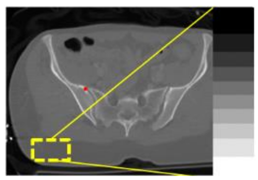	**$ASIS_{Lat}$ depth**, Lateral component of depth of SAT as measured along a vector from SI joint to ASIS in plane (R,L)	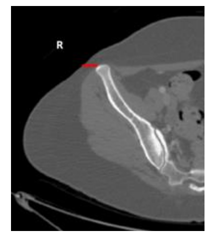
SAT area (mm^2), Cross sectional area of the segmented SAT	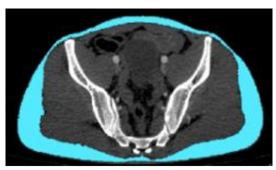	**$ASIS_{SI}$ depth**, Depth of SAT as measured along a vector from SI joint to ASIS in plane (R,L)	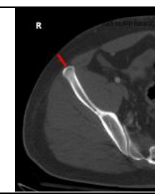
Linea alba depth (mm), Depth of SAT as measured in plane at the linea alba	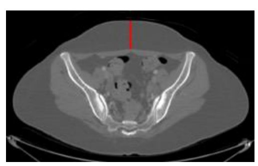	**L_{perp} diameter (mm)**, Length of the body in the anterior-posterior plane in the SAT segmentation plane	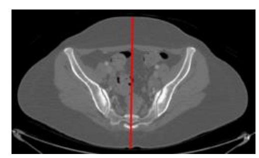
Rectus Abd. Depth, Depth of SAT as measured in plane at the rectus abdominis (R,L)	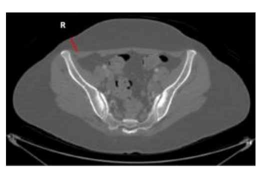	**L_{max} diameter (mm)**, Maximum length of the body in the L-R direction in the SAT segmentation plane	
Perimeter (mm), Length around the body in the SAT segmentation plane		**Maximum Linea Alba Depth differential**, Maximum difference of Depth at Linea Alba from measurement at the level of the ASIS	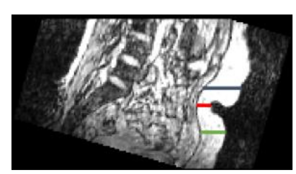

Quality Control

An additional step was required if the full SAT was not visible. This primarily occurred when the patient’s size exceeded the scan’s field of view (FOV). Examples of scans where a right or left flank is not in view can be found below in Figure 4.

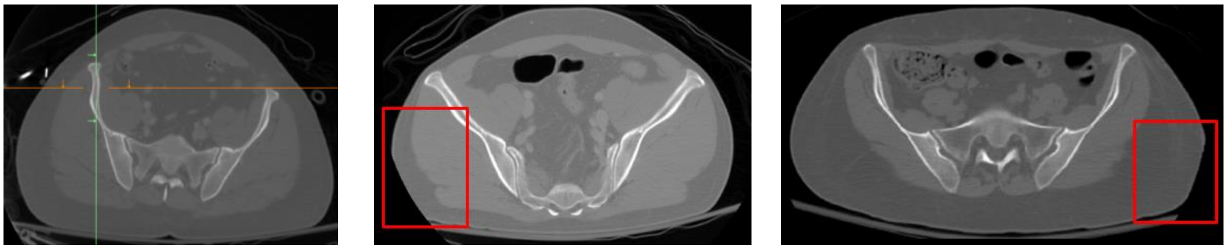

Both flanks in view Right flank clipped Left flank clipped

Figure 4. Examples of both flanks in view (left), compared to single flank in view. Clipped region is indicated by the red box.

In these cases, the protocol required the user to assume left-right symmetry. A midline axis of symmetry was assigned through the linea alba anteriorly and the middle of the sacrum posteriorly. Next, the area of SAT was measured on the aspect of the body that was fully within the FOV. The total area was then set equal to 2 times the visible area. A half-arc was measured from anterior to posterior on one side, beginning and ending at the midline, to determine perimeter, which was set as twice the half arc length. The anterior-posterior distance was measured at the midline and the lateral distance was set as twice the maximum observed distance from the midline to the lateral-most protrusion of the SAT. All other depth measures were taken per protocol, since no images were missing the right and left ASIS. Examples of the half symmetry method are shown in Figure 5.

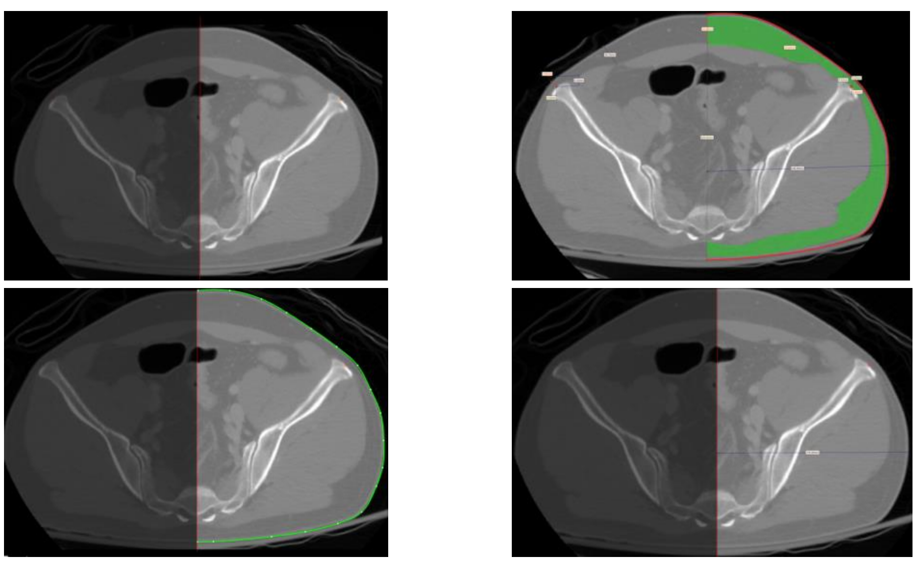

Figure 5. Half symmetry method to determine area and perimeter measures. Clockwise from top left, A-P distance in red, half area in green shaded, half lateral distance gray line, and half perimeter, green line.

Statistical Analysis

All outcome measures from supine CT were cross-plotted against measures from supine MRI to graphically assess how well analysis could be translated across image modality. Additionally, outcome measures from supine MRI were cross-plotted against measures from seated MRI to assess the effect of postural changes. Plots were created using Microsoft Excel (2016). A linear trend line was calculated for each plot. Slope, intercept, and R^2 values were used to determine correlation between scans. Wilcoxon signed-rank tests were performed in SAS (v. 9.4, Cary, NC) to determine if SAT measures yield statistically significant differences between modalities and postures. Measures with significance ($p < 0.05$) were noted. In addition, given the small sample size, measures approaching significance ($0.05 < p < 0.075$) were noted.

RESULTS

Image Analysis Results

The half symmetry analysis was utilized in 3 out of 18 scans, 2 of which from the same subject. All measures were not collected in 3 out of 18 scans for varying reasons. In one supine MRI scan, an external marker obstructed the view of the landmarks necessary for the right $ASIS_{SI}$, $ASIS_{Lat}$, and $ASIS_{Ant}$ measurements. In one seated MRI scan, the anterior portion of the SAT exceeds the field of view, so only the right and left $ASIS_{SI}$ and $ASIS_{Lat}$ measurements were collected. In one seated MRI scan, SAT area and quality measures are unavailable due to the full flank being out of view on both sides of the body. A fold in the SAT prevented measurement of the left $ASIS_{Lat}$ as well. Lumbar lordosis was only collected in the CT scans. Not enough of the anatomy was visible in MRI scans to include the measure and so it was not investigated further. HU data is also not included in the cross plots but is reported in the data in the Appendix. HU differences are a consequence of the different imaging modalities themselves, were anticipated, and are not related to the SAT depth changes observed which is the main focus of this work.

Sagittal Linea Alba

The results of the supplemental Linear Alba depth measures are shown below in Figure 6. Measurements were only collected on 5 subjects as the exterior portion of the SAT exceeds the FOV for one subject. The average Linea Alba depth taken per protocol was 17.82 mm while the average maximum deviation as seen in the sagittal plane was 14.83 mm. These supplemental measurements were taken 23.8 mm inferior/superior to the per protocol depth on average. Depth is more than doubled in 3 out of 5 subjects with the largest percentage increase seen in the small male (181%). Contrastingly, the large male only has an increase of 0.5%. However, for this scan the SAT fold was located lower in the abdomen than other scans such that the Linear Alba depth measured at the level of the ASIS is not within the fold.

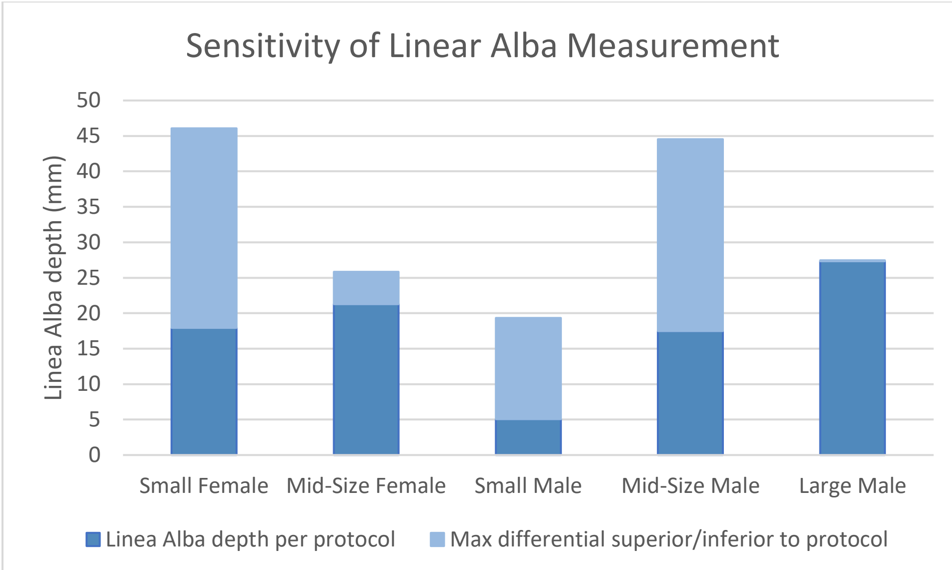

Figure 6. Supplemental measures of Linea Alba depth. Depth at ASIS as taken per protocol is shown in dark blue. Max differential from this depth is shown in blue if taken from the superior measure or shown in green if taken from the inferior measure.

Cross Plots

The main goals of this study were to evaluate how well supine CT correlates to supine MRI and to evaluate the effect of postural changes on the outcome measures. This was initially accomplished by cross plotting supine CT measurements with supine MRI measurements and by cross plotting supine and seated MRI measurements. All left and right measures were averaged prior to plotting since no difference was observed from left to right. The resulting slope and R^2 values are reported in Table 3.

Slopes closer to one with small y-intercept values indicate that the two measures are very similar, and a higher R^2 values indicates a more linear agreement. For supine CT and MRI, all measures have a slope and R^2 value near one and small y-intercepts, suggesting that SAT characteristics match well between image modality. When looking at postural changes, SAT area and perimeter had a slope and R^2 value near one like the supine scans. Measures of L_{max} diameter, L_{Perp} diameter, Linea Alba depth, and Rectus Abdominis depth had low R^2 values, slopes less than 1, and larger y-intercepts, suggesting that these measurements do not have a strong linear correlation from supine to seated posture. Measures of $ASIS_{SI}$ depth and $ASIS_{Ant}$ depth had higher R^2 values, but had slopes greater than one. This indicates that while linearly correlated, these measures are greater in seated posture than in supine posture.

Table 3. Summary of cross plot statistics for modality and posture comparisons

	CT vs MRI supine		MRI supine vs MRI seated	
Measure	**Slope**	**R^2**	**Slope**	**R^2**
SAT area (mm^2)	1.02	0.99	1.01	0.91
Perimeter (mm)	1.03	0.99	1.08	0.91
L_{max} diameter (mm)	1.02	0.99	0.76	0.65
L_{perp} diameter (mm)	0.93	0.85	0.64	0.38
Linea alba depth (mm)	0.89	1.00	0.35	0.68
$ASIS_{SI}$ depth	1.09	1.00	2.23	0.94
$ASIS_{Lat}$ depth	0.97	1.00	1.19	0.87
$ASIS_{Ant}$ depth	0.95	1.00	7.96	0.85
Rectus Abd. Depth	0.94	1.00	0.70	0.20

Slope Scale	0	0.5	1	1.5	2
R^2 Scale	0.25	0.5	0.75	0.9	1

Cross plots are shown below for $ASIS_{SI}$ depth (along the vector from the SI to the ASIS) for both supine CT vs supine MRI (Figure 7) and supine MRI vs seated MRI (Figure 8). As mentioned above, slope remains relatively unchanged for measures of SAT area for supine CT vs supine MRI (slope = 1.0196) to supine MRI vs seated MRI (slope = 1.0089). The y-intercepts of SAT are negligible (less than 6% of smallest area). While $ASIS_{SI}$ depth trends toward the identity line for scans of different modality and unchanged posture (slope = 1.0873), $ASIS_{SI}$ depth increases in seated posture (slope = 2.2271). Larger values of $ASIS_{SI}$ depth show a greater increase from supine to seated than smaller values.

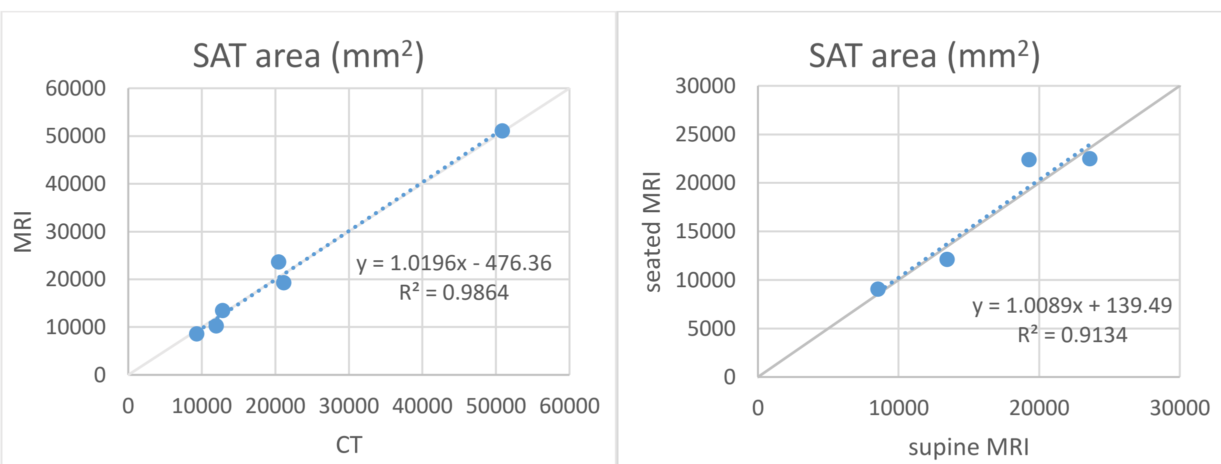

Figure 7. Cross plots for SAT area with modality comparison (left) and posture comparison (right). Identity line is shown in gray.

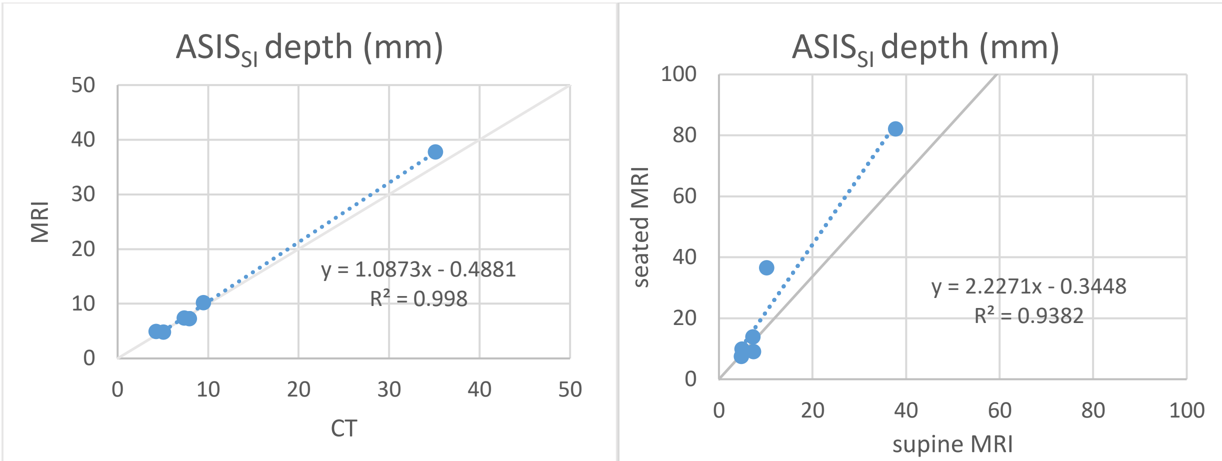

Figure 8. Cross plots for $ASIS_{SI}$ depth (along path from SI) area with modality comparison (left) and posture comparison (right). Identity line is shown in gray.

Signed-rank Tests

Signed-rank tests were conducted to compare SAT measures taken from matched supine CT, supine MRI, and seated MRI. The results of the tests are summarized in Table 4. Reported p-values were broken into three categories: significant ($p < 0.05$), approaching significance ($0.05 < p < 0.075$), and not significant ($p > 0.075$). Significant results indicate the difference between scans is not equal to zero. All left and right measures were averaged prior to testing since no difference was observed in left and right measures. If one left/right measure was unavailable, the available measure was used.

Table 4. Significance of each measure when comparing supine CT, supine MRI, and seated MRI. "A" indicates approaching significance, and "S" indicates significant. If not noted, the results were not significant. Bolded Variables showed significance or approached significance.

Categories of comparison	**CT v MRI**		**MRI v uMRI**		**CT v uMRI**	
Independent Variables	n	significance	n	significance	n	significance
SAT Area (mm^2)	6		4		4	
Perimeter (mm)	6		4		4	
L_{max} (mm)	6	**S**	4		4	
L_{perp} (mm)	6		4		4	
Linea alba depth (mm)	6		6		6	
$ASIS_{SI}$ depth (mm)	5		5	**S**	5	**A**
$ASIS_{Lat}$ depth (mm)	5		5		5	
$ASIS_{Ant}$ depth (mm)	5		5	**A**	5	
Rectus abdominis depth (mm)	6		5		5	

DISCUSSION

Measures of SAT were compared between image modality and posture. Cross plots of measures from supine CT and MRI show that the data trends along the identity line. Since posture is unchanged, this suggests that SAT characteristics are unaffected by image modality. In addition, when comparing supine CT to MRI through statistical tests using Wilcoxon signed-rank tests, only one measure, L_{max} was significant. Although statistically significant, it is likely a systematic difference and not clinically relevant. The in-plane resolution of the CT and MRI were nearly identical. It would follow that the perimeter and area would also be significantly different between CT and MRI given this finding, but they are not. These measures were not derived from L_{max} but rather from the mask (the collection of pixels) of SAT, which was readily visible in both scans. The difference is thought to be due to two factors. The first is based on sample. This comparison category (CT vs. MRI) contained L_{max} measures for 6 subjects, compared to only 4 in each of the other categories. The larger sample size combined with a relatively small variance leads to the identified statistical significance. The second is thought to be systematic, having to do with the pulse sequence used in collecting the MRI data. It is likely the border of the skin itself was somewhat harder to identify in the MRI because the boundaries between tissue types showed generally low signal by design to aid in segmentation. This is not the case in CT, which is based on x-ray projection.

Despite this observation, the percent change ranges from 0% to 3%, or no more than 5 mm. On the scale of the human body, this difference is thought to be inconsequential. If any bias is introduced in depth measures, they would be small and indicates that the true MRI thickness could be up to 3% larger than in a comparable CT. Further study may be needed to prove the above hypothesis. The main findings of the study hold despite this, ASIS depth along the SI joint regression slope was 2.2 times larger between MRI and seated MRI with differences in the 10's of mm, and both used the same pulse sequence to generate the images.

When comparing postural changes using supine and seated MRI, differences arise in several outcome measures. SAT area and perimeter remain the same despite changes in posture. However, ASIS depth measurements are higher in the seated MRI. The most significant difference is seen in the $ASIS_{Ant}$ measurement, suggesting that compared to supine position, SAT is distributed more anteriorly when seated. The signed rank tests found that in the postural change data, ASIS along the SI and anterior measures were significant or approached significance. The fact that the lateral measures did not indicate a difference, likely indicates a more anterior morphological rearrangement of the pannus.

Supplemental measurements of Linea Alba depth indicate sensitivity to the vertical distance at which the measurement is taken. Depending on how the SAT is distributed, it is possible for Linea Alba depth to double. These additional measurements were only taken in seated MRIs due to the presence of "SAT folds", but it would be interesting to expand these measurements to the supine scans as well to examine if this sensitivity is present in all postures.

This study provides quantitative measures of a key design variable: the thickness of the soft tissue envelope around bony prominences of the pelvis at the level of the ASIS. It further provides measures of thickness changes when subjects are in a seated posture. The interaction with restraint systems may be influenced by how much soft tissue surrounds bony prominences in the body and is affected by reclined postures. The results from this study highlight the shortcomings of using supine data to develop HBMs and ATDS in reclined settings and indicate a need for more data describing this area in the seated posture.

A limitation of this study is the fact that only 6 subjects were analyzed. A greater sample size would allow the evaluation of sex-based differences, further exploration of the association between outcome measures and BMI, and in general yield a more robust dataset. Many of the rank-sum tests did not yield statistically significant results. However, the cross plots clearly indicate a difference in several SAT depth measurements when moving from a supine to seated posture. Therefore, these results warrant further investigation.

Future work could leverage an additional 12 sets of scans at Wake Forest that are in triplicate, with CT, MRI and uMRI at a 90 degree seatback angle. Finally, future work could focus on the acquisition of additional uMRI data in the reclined MRI focused specifically on a change in seatback angle.

CONCLUSIONS

Despite the small sample size, the investigation yielded statistically significant results.

- SAT measurements correlate between CT and MRI when the subject is supine. Therefore, MRI data can be used to quantify SAT since it has been shown to be essentially equivalent to CT data, which is considered the gold standard given its high resolution and use in prior studies.
- Analysis methods developed for supine CT translate to seated MRI.
- While SAT area remains the same from supine to seated, depth measurements at the ASIS in the anterior direction and a vector along the SI joint show an increase when seated.
- The depth of SAT at the linea alba can more than double when compared to the depth at the ASIS, when analyzing several cm above and below the ASIS due to variations in the thickness of SAT in this area. These variations can occur naturally through the fold in the pannus or due to clothing.

ACKNOWLEDGEMENTS

Thank you to our colleagues and collaborators at Toyota Motor North America (Dr. Hallman) of the Collaborative Safety Research Center for his contribution and input on this project.

REFERENCES

Boyle, Kyle J, Matthew P Reed, Lauren W Zaseck, and Jingwen Hu. 2019. "A human modelling study on occupant kinematics in highly reclined seats during frontal crashes." In *Proceedings of the 2019 IRCOBI Conference. Florence, Italy*.

Gayzik, F Scott, Craig A Hamilton, Josh C Tan, Craig McNally, Stefan M Duma, Kathleen D Klinich, and Joel D Stitzel. 2009. "A multi-modality image data collection protocol for full body finite element model development." In.: SAE Technical Paper.

Gayzik, F.S., D. P. Moreno, K.A Danelson, C McNally, K.D. Klinich, and J. D. Stitzel. 2012. 'External Landmark, Body Surface, and Volume Data of a Mid-Sized Male in Seated and Standing Postures', *Annals of biomedical engineering*, 40: 2019-32.

Gayzik, F.S., D.M. Moreno, C.P. Geer, S.D. Wuertzer, R.S. Martin, and J.D. Stitzel. 2011. 'Development of a Full Body CAD Dataset for Computational Modeling: A Multi-Modality Approach', *Annals of biomedical engineering*, 39: 2568-83.

Gepner, B, D Draper, K Mroz, R Richardson, M Ostling, B Pipkorn, JL Forman, and JR Kerrigan. 2019. "Comparison of human body models in frontal crashes with reclined seatback." In *Proceedings of the 2019 IRCOBI Conference. Florance, Italy*.

Lamielle, Sophie, Sophie Cuny, Jean-Yves Foret-Bruno, Philippe Petit, P Vezin, Jean-Pierre Verriest, and Herve Guillemot. 2006. "Abdominal injury patterns in real frontal crashes: influence of crash conditions, occupant seat and restraint systems." In *Annual Proceedings/Association for the Advancement of Automotive Medicine*, 109. Association for the Advancement of Automotive Medicine.

Luet, Carole, Xavier Trosseille, Pascal Drazétic, Pascal Potier, and Guy Vallancien. 2012. "Kinematics and dynamics of the pelvis in the process of submarining using PMHS sled tests." In.: SAE Technical Paper.

Rawska, Katarzyna, Bronislaw Gepner, Shubham Kulkarni, Kalle Chastain, Junjun Zhu, Rachel Richardson, Daniel Perez-Rapela, Jason Forman, and Jason R Kerrigan. 2019. 'Submarining sensitivity across varied anthropometry in an autonomous driving system environment', *Traffic Inj Prev*, 20: S123-S27.

Richardson, Rachel, John Paul Donlon, Kalle Chastain, Greg Shaw, Jason Forman, Sara Sochor, Mohan Jayathirtha, Kevin Kopp, Brian Overby, and Bronislaw Gepner. 2019. "Test methodology for evaluating the reclined seating environment with human surrogates." In *26th International Technical Conference on the Enhanced Safety of Vehicles (ESV), In press*.

Uriot, Jérôme, Pascal Potier, Pascal Baudrit, Xavier Trosseille, Olivier Richard, and Richard Douard. 2015. "Comparison of HII, HIII and THOR dummy responses with respect to PMHS sled tests." In *Proceedings of IRCOBI Conference*.